Journal of Earth Science, *Vol. 35*, *No. 3*, *p. 1069−1074*, *June 2024* *ISSN 1674-487X*
Printed in China
https://doi.org/10.1007/s12583-024-2011-y

Editorial

Resonance Analysis in a High-Rise Building: Combined Translational and Rotational Measurements

Linpeng Qin [1], **Yun Wang** *[1], **Chang Chen**[1], **Yongxiang Wei**[2], **Chunqi Liao**[2], **Yi Zhang**[1], **Chao Wang**[3], **Wentao Wan**[1], **Quanyang Shao**[1]

1. *School of Geophysics and Information Technology*, *China University of Geosciences*, *Beijing* 100083, *China*
2. *Fujian Earthquake Agency*, *Fuzhou* 350003, *China*
3. *Institute of Geochemistry*, *Chinese Academy of Sciences*, *Guiyang* 550081, *China*

Linpeng Qin: https://orcid.org/0000-0003-2251-3811; Yun Wang: https://orcid.org/0000-0002-7543-4677

0 INTRODUCTION

Resonance frequency is an important indicator for structure health monitoring, which can be exacerbated by various natural forces, such as rainfall, earthquakes, and hurricanes (Wu et al., 2021; Shan et al., 2020; Gentile et al., 2016; Moser and Moaveni, 2011). Clinton et al. (2006) found that changes in environmental factors could significantly affect the resonance frequency of the Millikan Library; and that compared with temperature, humidity and strong wind have greater impacts on resonance frequency. Additionally, some studies have confirmed the effects of environmental factors through mathematical statistical analyses, including Xia et al. (2006), Yuen and Kuok (2010), and Guéguen et al. (2017). Other studies (e.g., Astorga et al., 2018) revealed a building's self-healing ability, where the building's resonance frequency drifts due to earthquake events, environmental factors, or random forced vibrations could gradually return to its original level, but the recovery time of frequency drift could be considerably different with respect to different environmental factors.

Current research on medium resonance modes mainly focuses on translational resonance, but we note that there is consensus that torsional motion (rotational motion around the vertical axis) contributes greatly to building damage (Guidotti et al., 2018; Guéguen et al., 2017). This highlights the necessity to reconsider the torsional effect during the construction and design of high-rise buildings that are susceptible to strong earthquakes, even for those with seemingly symmetric structures (Rossi et al., 2023, 2021; Guéguen and Astorga, 2021; Morelli et al., 2021; Bońkowski et al., 2019). Most knowledge about the torsion effects on tall buildings has derived from physical and mathematical simulations (e.g., Şafak, 1993). However, the increasing sensitivity of rotational seismometers in the past two decades has enabled the analysis of actual rotational motion of tall buildings through Structural Field Testing (SFT) and Structural Health Monitoring (SHM) (Murray-Bergquist et al., 2021), and leads to a series of meaningful researches. For instance, Guéguen et al. (2021) discovered that the rotation rate derived from the translational array is smaller than that recorded by a rotational seismometer when the center of torsion is not located at the same location. This finding facilitates the determination of the rotational center of the building. Bońkowski et al. (2021, 2019, 2018) found that the bending moments of high slender towers are significantly affected by the rotational motion of the ground, although under moderately intensive induced seismic events.

This study presents analyses of the characteristics of translational and torsional resonance of a high-rise building located in Xiamen City, China under ambient noise. We hope to have emphasized that rotational motion is distinct from translational motion and should be studied more, especially in high-rise buildings.

1 DATA AND METHODS

The high-rise building evaluated in this study which lies at Lujiang Road in Xiamen City, is a concrete-filled circular steel tubular structure, as illustrated in Figure 1. The design of the building includes a brace layout to mitigate the adverse effects of shear motion, and the standard floor plan of the structure is shown in Figure 1b (Du et al., 2012). The building has 43 floors above the ground level (192 m) and 5 floors below the ground level (21.2 m). The first floor is 9.0 m high and serves as a commercial space. The 14th and 24th floors are refuge floors that are 4.8 m high and have *Y*-oriented horizontal steel frames (Figure 1a). The remaining floors are standard office floors that are 4.2 m high.

A reference station for studying site effects is installed in a half-underground two-story brick-concrete hotel, which is approximately 100 m away from the high-rise building (Figure 1a). The hotel is built directly on the shallow sedimentary layer, with a burial depth of only 1 m. For the sake of simplicity, we refer to this location as the "site station" throughout the paper. The translational seismometers (CMG-3ESPCD, flat response frequency range: 0.016 7−50 Hz) were installed on the basement floor (-5th floor), middle floor (24th floor), and top floor (roof cabins, above 43rd floor) of the high-rise building

*Corresponding author: wangyun@mail.gyig.ac.cn
© China University of Geosciences (Wuhan) and Springer-Verlag GmbH Germany, Part of Springer Nature 2024

Manuscript received January 22, 2024.
Manuscript accepted February 25, 2024.

Qin Linpeng, Wang Yun, Chen Chang, Wei Yongxiang, Liao Chunqi, Zhang Yi, Wang Chao, Wan Wentao, Shao Quanyang, 2024. Resonance Analysis in a High-Rise Building: Combined Translational and Rotational Measurements. *Journal of Earth Science*, 35(3): 1069–1074. https://doi.org/10.1007/s12583-024-2011-y. http://en.earth-science.net

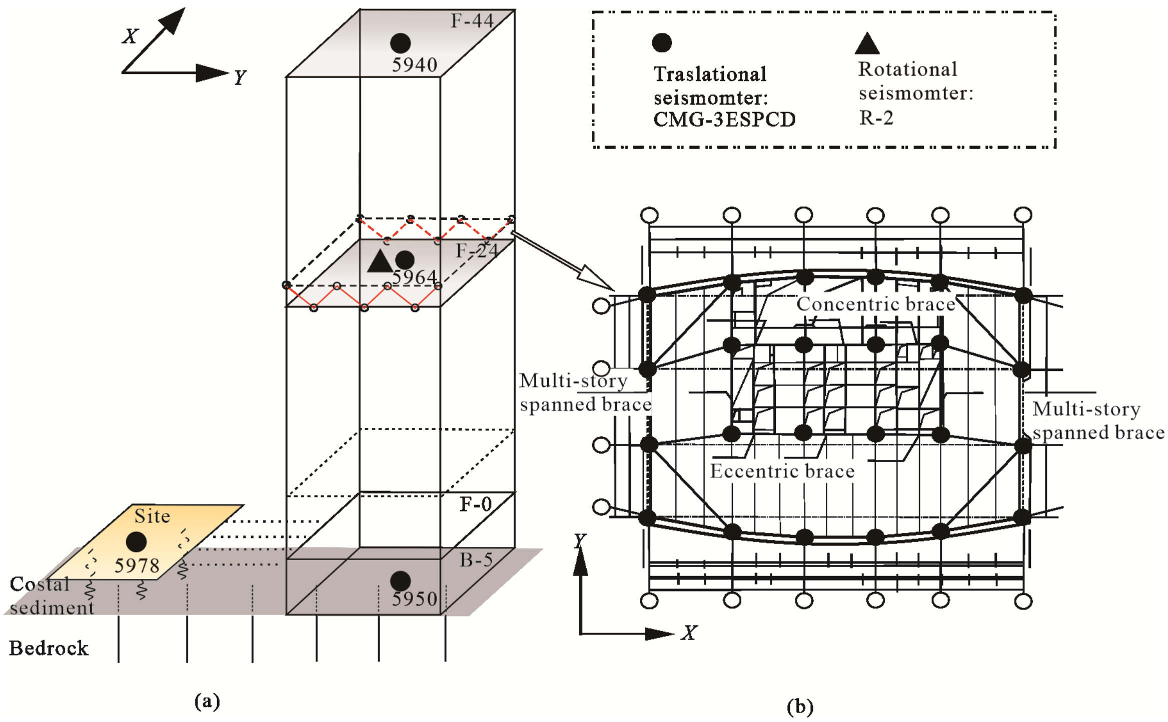

Figure 1. Sketch showing the basic information for the high-rise building (Du et al., 2012). (a) Instrument layout, the red line shown on the 24th floor represents the *Y*-oriented horizontal steel frame on the refuge floor. (b) Standard floor structure plan.

and have continuously recorded for at least 77 days, the rotational seismometer (R-2, flat response frequency range: 0.033 3–50 Hz) was installed on the middle floor of the building and has recorded for 15 days, and translational seismometers located at the site station have recorded for nearly 23 days.

Since the horizontal-to-vertical spectral ratio (HVSR) method was proposed by Nakamura (1989), many studies have proven that the method can be utilized to well identify the resonance frequency of the site or building (e.g., Guo et al., 2022; Stanko et al., 2016; Nath et al., 2005; Arai and Tokimatsu, 2004; Lermo and Chávez-García, 1993), which was calculated as

$$HVSR(f) = \sqrt{\frac{NS(f)^2 + EW(f)^2}{2V(f)^2}} \quad (1)$$

where $NS(f)$, $EW(f)$ and $V(f)$ represent the amplitude spectra of the NS, ES and vertical records from the translational seismometer, respectively.

To analyze the torsional motion responses of the high-rise building, we proposed the rotational vertical-to-horizontal spectral ratio (RVHSR) method based on the HVSR method, which takes the torsional motion of the high-rise building into account. The RVHSR can be calculated by the following formula

$$RVHSR(f) = \sqrt{\frac{2V_R(f)^2}{NS_R(f)^2 + EW_R(f)^2}} \quad (2)$$

where $NS_R(f)$, $EW_R(f)$ and $V_R(f)$ represent the amplitude spectra of the NS, ES and vertical rotational components from the rotational seismometer, respectively.

The single-station hourly HVSR and RVHSR spectra are obtained in 4 steps. First, the preprocessing of mean removal, trend removal, resampling, and bandpass filtering (0.1–10 Hz) are conducted on the raw data. And then, the Konno-Ohmachi method (Konno and Ohmachi, 1998) with a window length of 40 is adopted to smooth the amplitude spectrum. Subsequently, HVSR spectra and RVHSR spectra are calculated. Finally, since the seismic records at different floors are polluted by earthquake events, strong transients of human footsteps and some periods of recording are missed due to instrument power interrupts, the *K*-means method (Lloyd, 1982) is used to clean the raw HVSR spectra (Figure S1).

2 RESONANCES OF TRANSLATIONAL MOTION

A narrow peak with a high amplitude at around 3 Hz shows in the HVSR spectrum of the site station (Figure 2a), which is consistent with the theory of the site amplification effect of Xiamen's low-velocity soft coastal sediments with a thickness of about 20 m and the shear wave velocity of about 200 m/s (Fan et al., 2021). In contrast, the average HVSR spectrum of the basement shows a notch about 3 Hz, which suggests that the foundation design of the high-rise building reasonably avoids the possibility of site resonance. The average hourly HVSR spectra of the middle and top floors of the high-rise building show five resonance frequencies (Figures 2c, 2d) from approximately 0.277, 0.395, 0.85, 1.175 Hz, and to 1.65 Hz. For the convenience of description, these resonance frequency bands are defined as numbers F1, F2, F3, F4, and F5, respectively.

Variations of the HVSR spectra and the resonance frequency of the top floor with time are shown in Figure 3. The HVSR spectra value during the day is significantly larger than that at night in F1–F4. From the 30th day to the 35th day, corresponding to a reduction in human activities caused by the traditional Chinese Spring Festival, there are obvious low-amplitude HVSR spectra in F1–F3. These phenomena suggest that human

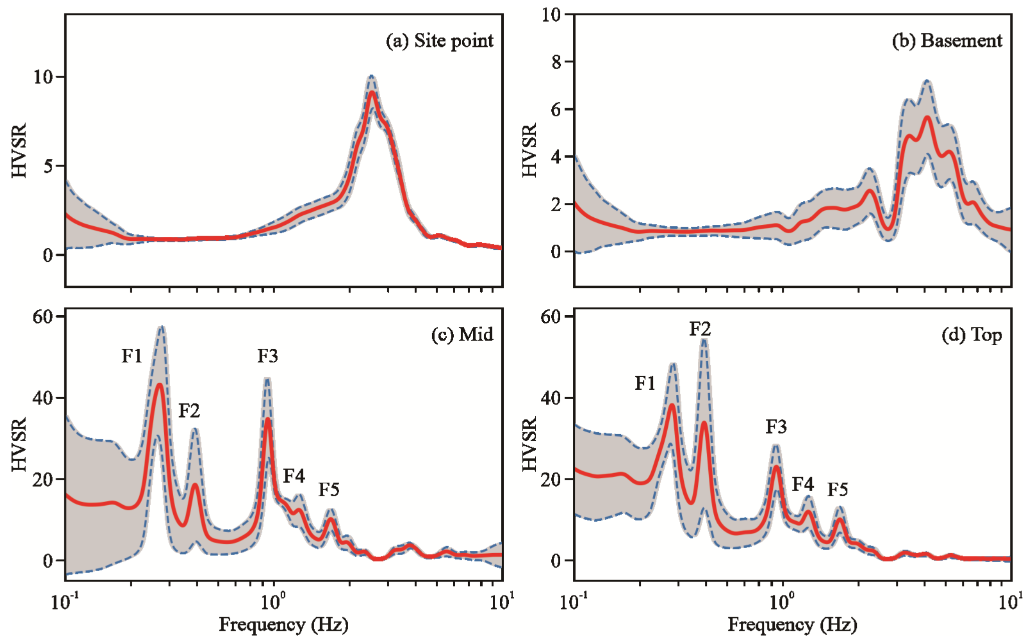

Figure 2. Average HVSR spectra (red line) and standard deviations (blue line and gray zone) for the site station (a), basement (b), middle floor (c), and top floor (d) of the high-rise building.

activities, particularly those inside the building, significantly strengthen the high-rise building's horizontal vibration below 1.2 Hz.

Figure 3f shows the climate data recorded by the local climate observatory during observation, which is located at a straight-line distance of less than 4 km from the building. The onset of precipitation is usually accompanied by an increase in humidity, resulting in a significant decrease of the resonance frequency F1 and an increase of the resonance frequency F2–F5.

Figures 3a–3e illustrate the resonance frequency variations of the top floor, where black dots represent nighttime data and white dots represent daytime data. Clear diurnal patterns emerge in the resonance frequencies of F1, F3, and F5 (Figures 3a, 3c, 3e, and 3g1). Notably, F1 shows a consistent decrease in resonance frequency during nighttime, while the resonance frequencies of F3 and F5 bands exhibit a continuous increase during the same period, with an obvious turning point at off-duty time (18 : 00 Beijing time). Furthermore, such diurnal variation of the resonance frequency becomes less obvious during the traditional Chinese Spring Festival (Figure 3g1, 30–35 days), indicating that the main factor affecting the diurnal variation of the resonance frequency is human activity rather than temperature. However, the resonance frequencies of the F2 and F4 do not show any significant diurnal variations (Figures 3b, 3d and 3g2), which implies that human activities have different impacts on different resonance modes (Chen et al., 2023).

Variations of the resonance frequencies of the middle floor (Figure S2) are similar to those of the top floor, but the resonance frequency F1 (Figure 4e) is lower than that of the top floor (Figure 3e), and the resonance frequency of F3 (Figure S2c) is higher than that of the top one (Figure 3c).

3 RESONANCES OF TORSIONAL MOTION

The average hourly RVHSR spectra of the middle floor of the high-rise building reveal three distinct torsional resonance frequencies (Figure 4) at approximately 0.395, 1.115 and 2.175 Hz. The first two resonance frequencies fall within the F2 and F4 frequency bands (Figure 3); and the higher resonance frequency at 2.175 Hz, is defined as F6.

The amplitudes of the RVHSR spectra change diurnally on weekdays (Figure 5), with higher amplitudes during the day than at night. However, the torsional resonance frequencies do not exhibit diurnal changes, which implies that human activities have no obvious impact on the torsional resonance frequencies of the high-rise building.

4 CONCLUSIONS

We conducted a preliminary analysis of six-component seismic records observed in a high-rise building in Xiamen and arrived at the following conclusions. Firstly, the translational components' horizontal-to-vertical spectral ratios (HVSRs) displayed five resonance modes (F1 = 0.277 Hz, F2 = 0.395 Hz, F3 = 0.85 Hz, F4 = 1.175 Hz, and F5 = 1.65 Hz) at the middle and top floors. Secondly, using rotational vertical-to-horizontal spectral ratios (RVHSRs) of rotational components, we identified three torsional resonance modes at the middle floor, two of which overlapped with the translational resonance frequencies F2 and F4, indicating the superposition of torsional and translational modes. Another relatively weak resonance mode occurred at F6 = 2.175 Hz, which was only detected by the rotational seismometer. The amplitude decreased as the frequency band increased in both translational and rotational resonance modes.

Furthermore, average hourly HVSR spectra and RVHSR spectra under ambient noise indicated that the resonance frequencies were affected by environmental and human factors. Environmental factors significantly impacted all resonance frequencies. The resonance frequency drift caused by the first rainfall lasted for a few days, but slowly recovered since the end of rainfall. The translational resonance frequencies (F1, F3, and F5) were significantly affected by human activities. The reso-

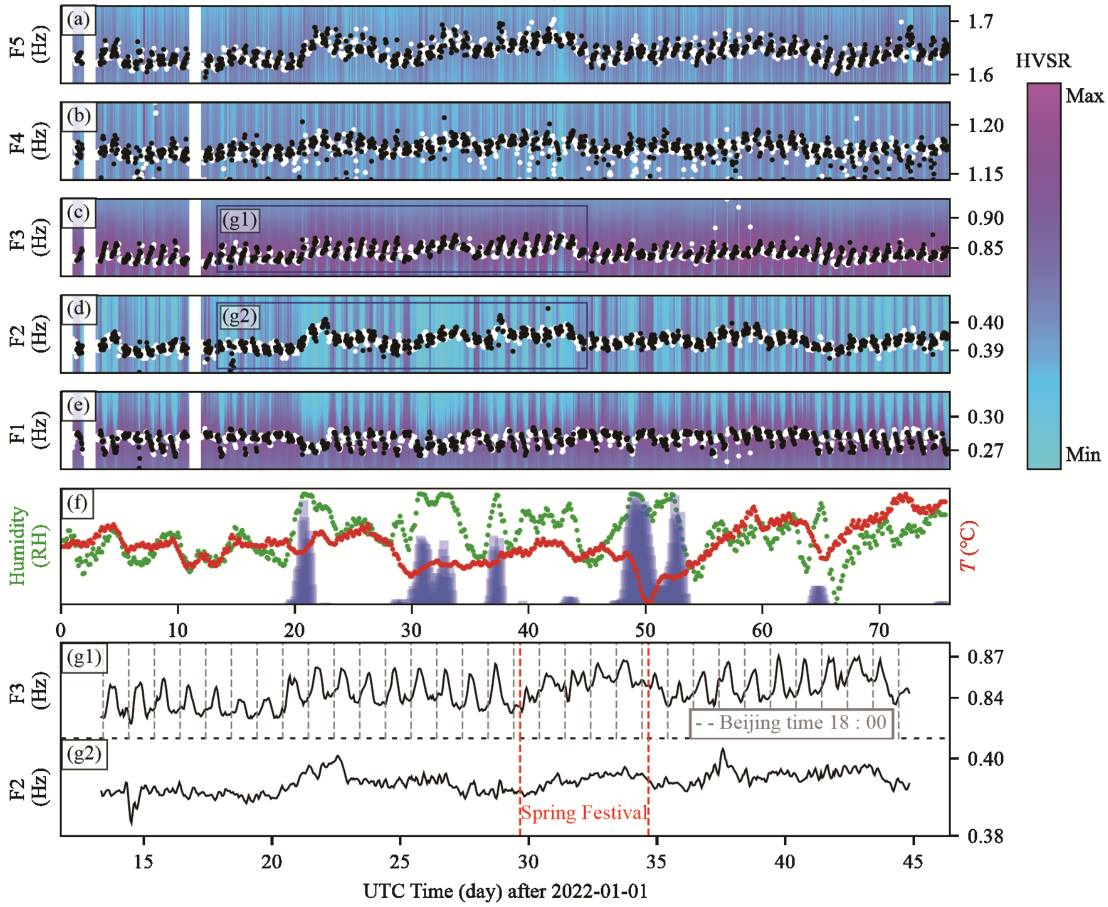

Figure 3. (a)–(e) HVSR spectra and resonance frequencies of F1, F2, F3, F4, and F5 frequency bands of the top floor with time. The hourly HVSR spectra of each frequency band are represented in the background. Black dots in (a)–(e) represent the resonance frequency changes at night, and white dots represent the resonance frequency changes during the day. The vertical white part in (a)–(e) represents missing data. (f) Normalized climate data recorded by weather stations. Rainfall data is represented by the histogram. (g1) The resonance frequency in F3 (dark blue rectangle in c) (g2). The resonance frequency in F4 (dark blue rectangle in (d).

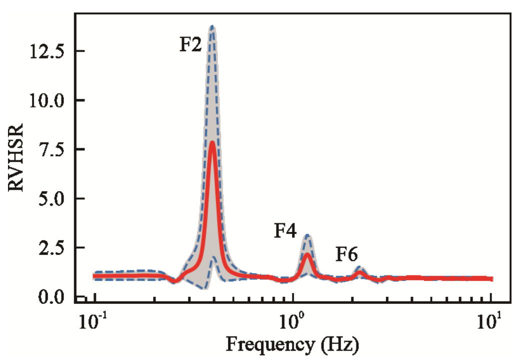

Figure 4. Average RVHSR spectrum (red line) and standard deviation (blue line and gray zone) for the middle floor.

nance frequencies in F3 and F5 decreased while the resonance frequency in F1 increased during the day, and vice versa. The torsional resonance frequencies (F2 and F4) were not affected by human activities. The resonance frequencies (F2 and F4) containing rotational components do not show a diurnal variation pattern, which represents the different physical mechanisms of the building's translational motion and torsional motion.

Six-degree-of-freedom monitoring on geoengineering projects, such as high-rise buildings or bridges, increase with the development of rotational or six-component seismometers. This paper is a typical case of data-driven science, which provides results that can be informative for other structural health monitoring of high-rise buildings, especially with respect to the phenomenon of inconsistent effects of human activities on torsional and translational resonance frequencies. In addition, some theoretical and simulation work will be performed in the future, focusing on the theoretical differences between the translational resonance frequency and the torsional engineering frequency of tall buildings.

ACKNOWLEDGMENTS

We are grateful to the staff of the high-rise building for helping with the deployment of seismometers. This research was supported by the National Natural Science Foundation of China (Nos. 42150201, U1839208, 62127815), the Guizhou Provincial Science and Technology Projects (No. ZK[2023] key053). The final publication is available at Springer via https://doi.org/10.1007/s12583-024-2011-y.

Electronic Supplementary Materials: Supplementary materials (Figures S1–S2) are available in the online version of this article athttps://doi.org/10.1007/s12583-024-2011-y.

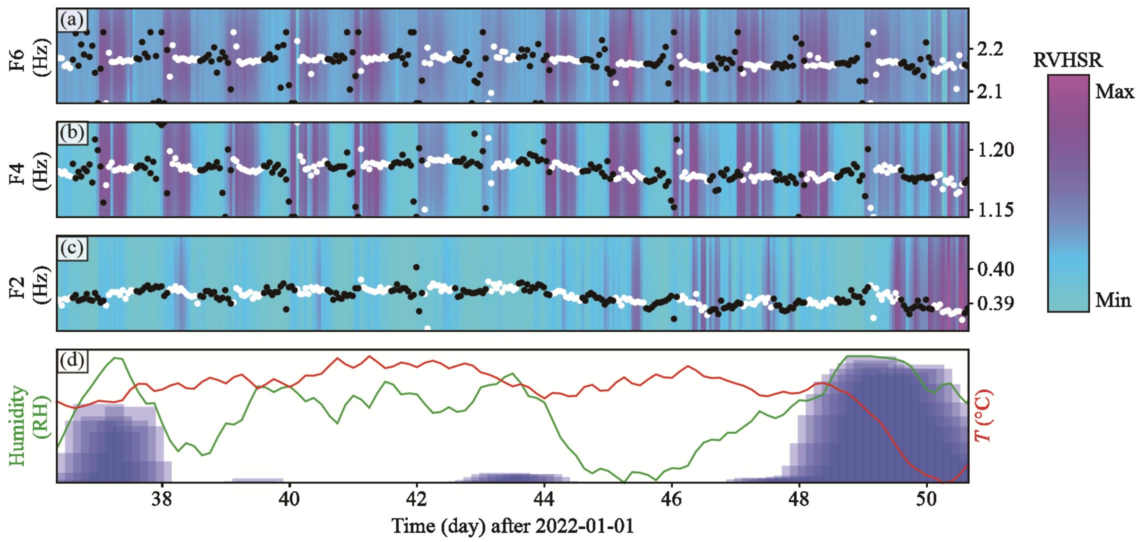

Figure 5. (a)–(c) RVHSR spectra and resonance frequencies of F2, F4, and F6 frequency bands of the middle floor with time. (d) Normalized climate data recorded by weather stations. Rainfall data is represented by the histogram.

Conflict of Interest

The authors declare that they have no conflict of interest.

REFERENCES CITED

Arai, H., Tokimatsu K., 2004. S-Wave Velocity Profiling by Inversion of Microtremor H/V Spectrum. *The Bulletin of the Seismological Society of America*, 94(1): 53–63. https://doi.org/10.1785/0120030028

Astorga, A., Guéguen, P., Kashima, T., 2018. Nonlinear Elasticity Observed in Buildings during a Long Sequence of Earthquakes. *Bulletin of the Seismological Society of America*, 108(3A): 1185–1198. https://doi.org/10.1785/0120170289

Bońkowski, P. A., Kuś, J., Zembaty, Z., 2021. Seismic Rocking Effects on a Mine Tower under Induced and Natural Earthquakes. *Archives of Civil and Mechanical Engineering*, 21(2): 65. https://doi. org/10.1007/s43452-021-00221-7

Bońkowski, P. A., Zembaty, Z., Minch, M. Y., 2018. Time History Response Analysis of a Slender Tower under Translational-Rocking Seismic Excitations. *Engineering Structures*, 155: 387–393. https://doi.org/10.1016/j.engstruct.2017.11.042

Bońkowski, P. A., Zembaty, Z., Minch, M. Y., 2019. Engineering Analysis of Strong Ground Rocking and Its Effect on Tall Structures. *Soil Dynamics and Earthquake Engineering*, 116: 358–370. https://doi.org/10.1016/j.soildyn.2018.10.026

Chen, Y., Guéguen, P., Chen, K. H., et al., 2023. Dynamic Characteristics of TAIPEI 101 Skyscraper from Rotational and Translation Seismometers. *Bulletin of the Seismological Society of America*, 113(2): 690–709. https://doi.org/10.1785/0120220147

Clinton, J. F., Bradford, S. C., Heaton, T. H., et al., 2006. The Observed Wander of the Natural Frequencies in a Structure. *Bulletin of the Seismological Society of America*, 96(1): 237–257. https://doi.org/10.1785/0120050052

Du, G., Wang, X. F., Xu, Z., 2012. Structural Design of Xiamen Fortune Centre. *Building Structure*, 42(4): 38–43. https://doi.org/10.19701/j.jzjg.2012.04.005 (in Chinese with English Abstract)

Fan, Z., Zhang, K. W., Zhang, Y. S., et al., 2021. Study on Apparent Wave Velocity Calculation Method and on Travelling Wave Effect. *Engineering Mechanics*, 38(6): 47–61 (in Chinese with English Abstract)

Gentile, C., Guidobaldi, M., Saisi, A., 2016. One-Year Dynamic Monitoring of a Historic Tower: Damage Detection under Changing Environment. *Meccanica*, 51(11): 2873–2889. https://doi.org/10.1007/s11012-016-0482-3

Guéguen, P., Astorga, A., 2021. The Torsional Response of Civil Engineering Structures during Earthquake from an Observational Point of View. *Sensors*, 21(2): 342. https://doi.org/10.3390/s21020342

Guéguen, P., Guattari, F., Aubert, C., et al., 2021. Comparing Direct Observation of Torsion with Array-Derived Rotation in Civil Engineering Structures. *Sensors*, 21(1): 142. https://doi.org/10.3390/s21010142

Guéguen, P., Langlais, M., Garambois, S., et al., 2017. How Sensitive are Site Effects and Building Response to Extreme Cold Temperature? the Case of the Grenoble's (France) City Hall Building. *Bulletin of Earthquake Engineering*, 15(3): 889–906. https://doi.org/10.1007/s10518-016-9995-3

Guidotti, R., Castellani, A., Stupazzini, M., 2018. Near-Field Earthquake Strong Ground Motion Rotations and Their Relevance on Tall Buildings. *Bulletin of the Seismological Society of America*, 108(3A): 1171–1184. https://doi.org/10.1785/0120170140

Guo, Z., Xue, M., Aydin, A., et al., 2022. Locating the Source Regions of the Single and Double-Frequency Microseisms to Investigate the Source Effects on HVSR in Site Effect Analysis. *Journal of Earth Science*, 33(5): 1219–1232. https://doi.org/10.1007/s12583-021-1501-4

Konno, K., Ohmachi, T., 1998. Ground-Motion Characteristics Estimated from Spectral Ratio between Horizontal and Vertical Components of Microtremor. *Bulletin of the Seismological Society of America*, 88(1): 228–241. https://doi.org/10.1785/bssa0880010228

Lermo, J., Chávez-García, F. J., 1993. Site Effect Evaluation Using Spectral Ratios with only one Station. *The Bulletin of the Seismological Society of America*, 83(5): 1574–1594. https://doi.org/10.1785/bssa0830051574

Lloyd, S., 1982. Least Squares Quantization in PCM. *IEEE Transactions on Information Theory*, 28(2): 129–137. https://doi.org/10.1109/tit.1982.1056489

Morelli, A., Zaccarelli, L., Cavaliere, A., et al., 2021. Normal Modes of a Medieval Tower Excited by Ambient Vibrations in an Urban Environment. *Seismological Research Letters*, 93(1): 315–327. https://doi.org/10.1785/0220210038

Moser, P., Moaveni, B., 2011. Environmental Effects on the Identified

Natural Frequencies of the Dowling Hall Footbridge. *Mechanical Systems and Signal Processing*, 25(7): 2336–2357. https://doi. org/10.1016/j.ymssp.2011.03.005

Murray-Bergquist, L., Bernauer, F., Igel, H., 2021. Characterization of Six-Degree-of-Freedom Sensors for Building Health Monitoring. *Sensors*, 21(11): 3732. https://doi.org/10.3390/s21113732

Nakamura, Y., 1989. Method for Dynamic Characteristics Estimation of Subsurface Using Microtremor on the Ground Surface. *Quarterly Report of RTRI* (*Railway Technical Research Institute*) (*Japan*), 30(1): 25–33

Nath, S. K., Vyas, M., Pal, I., et al., 2005. A Seismic Hazard Scenario in the Sikkim Himalaya from Seismotectonics, Spectral Amplification, Source Parameterization, and Spectral Attenuation Laws Using Strong Motion Seismometry. *Journal of Geophysical Research* (*Solid Earth*), 110(B1): B01301. https://doi.org/10.1029/2004jb003199

Rossi, Y., Tatsis, K., Awadaljeed, M., et al., 2021. Kalman Filter-Based Fusion of Collocated Acceleration, GNSS and Rotation Data for 6C Motion Tracking. *Sensors*, 21(4): 1543. https://doi. org/10.3390/s21041543

Rossi, Y., Tatsis, K., Clinton, J., et al., 2023. A New Paradigm for Structural Characterization, Including Rotational Measurements at a Single Site. *Bulletin of the Seismological Society of America*, 113(6): 2249–2274. https://doi.org/10.1785/0120230026

Şafak, E., 1993. Response of a 42-Storey Steel-Frame Building to the M_s = 7.1 Loma Prieta Earthquake. *Engineering Structures*, 15(6): 403–421. https://doi.org/10.1016/0141-0296(93)90059-d

Shan, J. Z., Zhang, H. Q., Shi, W. X., et al., 2020. Health Monitoring and Field-Testing of High-Rise Buildings: A Review. *Structural Concrete*, 21(4): 1272–1285. https://doi.org/10.1002/suco.201900454

Stanko, D., Markušić, S., Strelec, S., et al., 2016. Seismic Response and Vulnerability of Historical Trakošćan Castle, Croatia Using HVSR Method. *Environmental Earth Sciences*, 75(5): 368. https://doi. org/10.1007/s12665-015-5185-x

Wu, X. Y., Guo, Z., Liu, L. B., et al., 2021. Seismic Monitoring of Super High-Rise Building Using Ambient Noise with Dense Seismic Array. *Seismological Research Letters*, 92(1): 396–407. https://doi. org/10.1785/0220200119

Xia, Y., Hao, H., Zanardo, G., et al., 2006. Long Term Vibration Monitoring of an RC Slab: Temperature and Humidity Effect. *Engineering Structures*, 28(3): 441–452. https://doi.org/10.1016/j.engstruct.2005.09.001

Yuen, K. V., Kuok, S. C., 2010. Ambient Interference in Long-Term Monitoring of Buildings. *Engineering Structures*, 32(8): 2379–2386. https://doi.org/10.1016/j.engstruct.2010.04.012